Liquid Crystals

Publication details, including instructions for authors and subscription information:
http://www.informaworld.com/smpp/title~content=t713926090

Novel intermediate phases in an ionic fluorocarbon surfactant/water system

S. Puntambekar; M. C. Holmes; M. S. Leaver

To cite this Article Puntambekar, S. , Holmes, M. C. and Leaver, M. S.(2000) 'Novel intermediate phases in an ionic fluorocarbon surfactant/water system', Liquid Crystals, 27: 6, 743 — 747

To link to this Article: DOI: 10.1080/026782900202219

URL: http://dx.doi.org/10.1080/026782900202219

Liquid Crystals, 2000, Vol. 27, No. 6, 743–747

Novel intermediate phases in an ionic fluorocarbon surfactant/water system

S. PUNTAMBEKAR, M. C. HOLMES* and M. S. LEAVER

Centre for Material Science, Department of Physics, Astronomy and Mathematics,
University of Central Lancashire, Preston PR1 2HE, UK

(*Received 14 October 1999; accepted 20 December 1999*)

This small angle X-ray scattering study of the lyotropic phases in the binary tetramethylammonium perfluorodecanoate/water system shows that there are no classical lyotropic mesophases present. Much of the liquid crystal region is taken up with a random mesh intermediate phase, $Mh_1(0)$ and a phase with rhombohedral symmetry which is probably a rhombohedral mesh intermediate phase, $Mh_1(R\bar{3}m)$. This behaviour is unusual since previously these mesh phases have been associated with hydrocarbon surfactants or diblock copolymer melts. All the mesophases found have non-uniform interfacial curvature and a sufficiently strong inter-layer interaction to ensure the long range correlation of structures in some phases.

1. Introduction

Short perfluoroalkyl chain surfactants differ from their hydrocarbon analogues in being more hydrophobic and having a higher probability of taking up a rigid, all-*trans*-conformation [1]. The latter is due to the larger ionic radius of the fluorine giving a higher energy barrier to *cis*-conformations. In concentrated aqueous mixtures these surfactants tend to exhibit rather simple phase diagrams [2–4].

A systematic study of the caesium perfluoroalkanoate systems (C_7–C_{10} chain lengths) [3–7] has revealed a certain sequence of transitions: isotropic to discoidal nematic and then to lamellar phase with increasing surfactant concentration. The latter phase is not the classical lamellar phase with continuous extended bilayers, but one in which the bilayer is pierced by disordered water-filled pores. Increasing the perfluoroalkyl chain length simply shifts the phase transitions to higher temperatures whilst preserving the general form of the phase diagram.

The lithium perfluoro-octanoate (C_8 Li)/water system is unusual in that the first liquid crystalline phase that it forms on increasing the surfactant concentration from the micellar phase is a hexagonal phase, H_1. At higher surfactant concentrations it was found to exhibit an intermediate phase with a tetragonal mesh structure [8]. This is a layered structure with water-filled defects correlated between the layers. The analogous system, lithium perfluorononanoate (C_9 Li) does not show a tetragonal phase although it does exhibit a hexagonal phase. The formation of H_1 and tetragonal phases takes place despite the reluctance of fluorocarbon surfactants to form curved interfaces because of the restricted conformational range of short perfluoroalkyl chains. These observations for the lithium counter-ion are explained by the highly hydrated nature of the lithium ion and its being more difficult to bind to the interface. Electrostatic repulsion between the head groups introduces curvature into the phase structures.

The phase behaviour of two tetramethylammonium (TMA) salts in water has been studied. These are the perfluoro-octanoate (C_8) [9] and perfluorononanoate (C_9) systems [10]. Both phase diagrams feature an extensive lamellar phase existing at high surfactant concentrations and low temperatures. The high stability of the lamellar phase was explained in terms of the tetramethylammonium counter-ion being more closely associated with the bilayer. The greater association would lower electrostatic repulsion between head groups and favour a flatter interface. The C_9TMA/water system exhibits a discoidal nematic phase, not observed in the C_8TMA/water system. In addition it was discovered that the transition temperatures in the case of C_9TMA were 40°C higher than those observed with C_8TMA, suggesting that there may in fact be a nematic phase present at low temperatures and low surfactant concentrations in the latter system.

Recently we published a study of several short chain perfluorocarbon surfactants with unusual phase behaviour (they exhibited pseudo-lower consolute behaviour) [11]. This behaviour and the unusually thin bilayers (< length of one all-*trans*-perfluoroalkyl chain) was attributed

---

*Author for correspondence; e-mail: m.c.holmes@uclan.ac.uk

Liquid Crystals ISSN 0267-8292 print/ISSN 1366-5855 online © 2000 Taylor & Francis Ltd
http://www.tandf.co.uk/journals

to the tight binding of the tetrabutylammonium (TBA) counter-ion and the partial solvation of the counter-ion's butyl chains into the bilayer region. We have made a study of the phase structure and behaviour of a homologus series of C_{10} carboxylic surfactants in which the hydrophobicity of the counter-ion was progressively reduced by the substitution of butyl chains by methyl groups. The end point of this series was C_{10}TMA. Despite its similarity with previously studied systems, it shows some remarkable phase structures and raises fundamental questions about why simple binary mixtures of a simple surfactant and water have a propensity to form interfaces with non-uniform surface curvature.

2. Results

The tetramethylammonium perfluorodecanoate used in these experiments was synthesized by the neutralization of nonadecafluorodecanoic acid with tetramethylammonium hydroxide; the details are the subject of a paper in preparation. The C_{10}TMA was recrystallized and judged pure by microanalysis. A representation of the phases of the $C_{10}TMA/{}^2H_2O$ system is shown in figure 1, in the concentration range 20 to 90% by weight of surfactant and temperature range 0 to 100°C. The phase representation was obtained using optical polarizing microscopy and ^2H NMR spectroscopy of the solvent ^2H_2O. Initially it appeared unremarkable and to follow the pattern generic with this type of surfactant–water system. At high temperature and low surfactant concentration above the diagonal AA′ (figure 1), was an isotropic micellar phase, L_1. At low temperature and high surfactant concentration below the diagonal line AA′ (figure 1) was a lamellar phase. The L_1 and lamellar regions, $Mh_1(R\bar{3}m)$ and $Mh_1(0)$, are divided by a narrow lyotropic nematic phase, N_D probably of disk-shaped micelles which is separated from the L_1 phase by a two phase region. No samples were investigated above 90% by weight of surfactant although it is likely that there is a crystalline phase here.

Small angle X-ray scattering (SAXS) using the Daresbury Synchrotron source (2.1) showed that the lamellar-type phase region had a more complex and interesting structure. Figures 2 and 3 show a series of scattering curves taken at fixed concentration (70% by weight of surfactant) and at fixed temperature (25°C), respectively. It is clear that the lamellar region is not a simple lamellar phase.

In the region labelled $Mh_1(R\bar{3}m)$ in figure 1, the SAXS shows a multiple line scattering pattern with typically eight or nine sharp lines, figure 2 (e.g. 0°C). (The notation $Mh_1(R\bar{3}m)$ and $Mh_1(0)$ used here is fully explained in [12].) These lines can only be indexed to a structure with a rhombohedral symmetry. A detailed discussion of the modelling of $R\bar{3}m$ mesh phases is contained in [13]. The highest symmetry structure which fits with the observed lines is $R\bar{3}m$ see table 1.

This indexation is consistent with a number of possible structures, including a three-connected mesh which can be planar or puckered or can have connections between the layers to form a bicontinuous structure which is a rhombohedral distortion of a cubic structure. It will also fit a six-connected plane mesh. The detailed analysis of these structures is beyond the scope of this letter but is addressed in [13]. However, because of the obvious

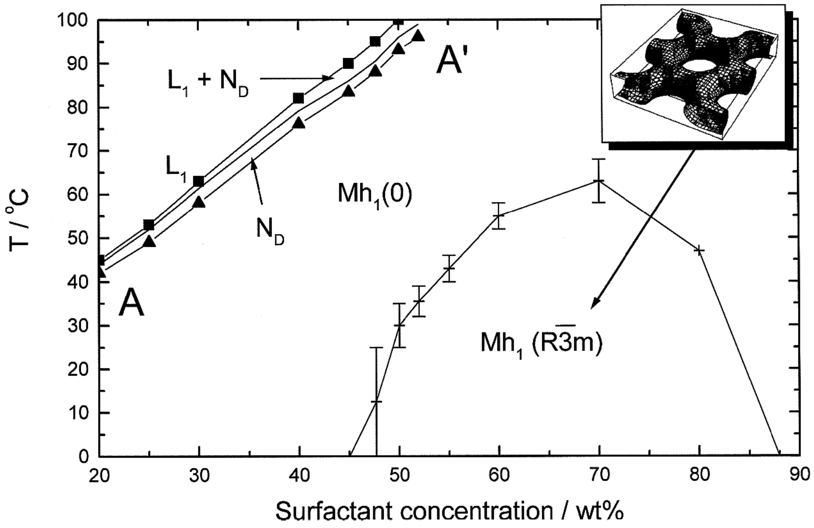

Figure 1. A representation of the phase diagram for the tetramethylammonium perfluorodecanoate/water system. $Mh_1(R\bar{3}m)$ is the rhombohedral mesh intermediate phase, $Mh_1(0)$ is the random mesh phase, N_D is a nematic phase which is probably made up of disk shaped micelles and L_1 is the isotropic micellar phase. The inset shows the supposed structure of one layer of the $Mh_1(R\bar{3}m)$ phase which contains water-filled pores arranged on a two dimensional hexagonal lattice. Error bars indicate the uncertainty in locating the phase boundary.

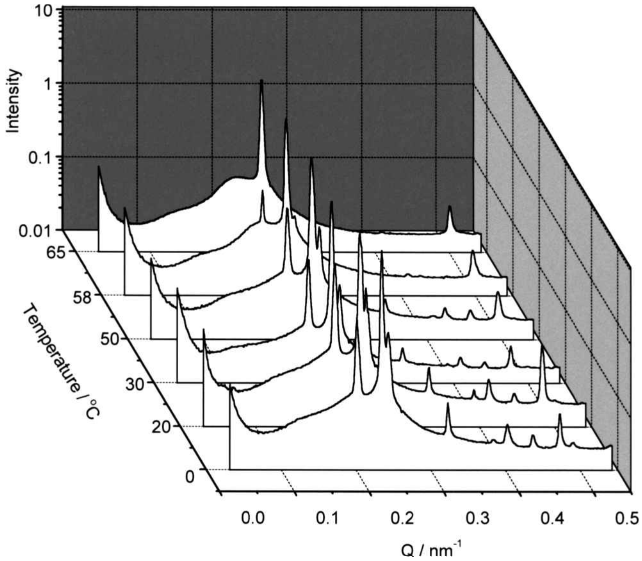

Figure 2. A series of SAXS curves taken from a 70% by weight (C_{10}TMA)/water sample at temperatures 0, 20, 30, 50, 58 and 65°C. Note that the temperature scale is not linear.

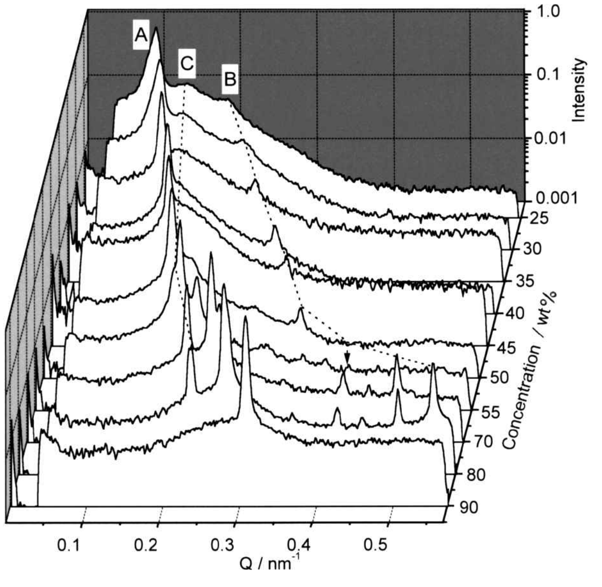

Figure 3. SAXS curves taken at a temperature of 25°C from a series of (C_{10}TMA)/water samples at 25, 30, 35, 40, 45, 50, 55, 70, 80, and 90% by weight. Note that the concentration scale is not linear. A and B indicate the first and second order of the layer repeat distance, whilst C represents the peak from the intra-planar structure in the $Mh_1(0)$ phase and from the (1 0 1) plane in the $Mh_1(R\bar{3}m)$ phase. The dotted lines have been added to help the eye.

Table 1. Indexation of 70% $C_{10}TMA/^2H_2O$ at 0°C to a $R\bar{3}m$ symmetry using the equation $1/d^2 = 4/3\,(h^2 + hk + k^2)/a^2 + l^2/c^2$. The lattice parameters a and c are taken from the (1 0 1) and (0 0 3) lines, respectively, and in this case have values of $a = 6.23$ nm and $c = 12.81$ nm (i.e. a layer spacing of 4.27 nm) and a ratio $c/a = 2.07$.

h	k	l	d_{obs}/nm	d_{cal}/nm
1	0	1	4.97	4.97
0	0	3	4.27	4.27
0	1	2	4.10	4.13
1	1	0	3.10	3.12
0	2	1	2.60	2.64
2	0	2	2.48	2.49
0	1	5	2.29	2.31
0	2	4	2.04	2.06
0	0	6	2.11	2.14

layer-like behaviour of the phase when viewed in the microscope, its proximity to the random mesh phase and its similarity to other surfactant water systems, its structure is probably a three-connected mesh structure in which the bilayer is pierced by water-filled holes which, within the bilayer plane, are arranged on a hexagonal lattice—see figure 1. The holes in adjacent layers are correlated in an ABC type packing. This type of structure has been observed in diblock copolymer melts [14–16] and more recently has been identified as an intermediate phase structure in non-ionic surfactant water mixtures, $C_{30}EO_9/^2H_2O$ and $C_{16}EO_6/^2H_2O$ [13, 17–19].

The structure varies very little with temperature at fixed surfactant concentration as illustrated by figure 2 and table 2, the slight decrease in a and c reflecting the increased perfluoroalkyl chain mobility and flexibility with elevated temperature. There are significant changes in the lattice parameters with concentration—see figure 3 and table 3. Increasing the water content increases the lattice parameters as expected, but the increase in c/a shows that the layer spacing increases more rapidly than the increase in the hole separation within the bilayer planes. This can be seen directly from the experimental evidence of figure 3 where both the layer reflection (A) and its second order (B) move significantly with changes in concentration, whereas the (1 0 1) reflection and the corresponding broad peak from the intra-planar order in the $Mh_1(0)$ phase (C) change very little.

Table 2. The variation of a, c and c/a with temperature for 70% $C_{10}TMA/^2H_2O$. The lattice parameters a and c were calculated as in table 1.

Temperature/°C	a/nm	c/nm	c/a
0	6.23	12.81	2.06
25	6.01	12.44	2.07
50	5.87	12.20	2.08
58	5.82	12.16	2.09
62	5.78	12.16	2.10

Table 3. The variation of *a*, *c* and *c/a* with concentration for $C_{10}TMA/^{2}H_2O$ at 25°C. The lattice parameters *a* and *c* were calculated as in table 1.

Concentration/% weight of C_{10}TMA	*a*/nm	*c*/nm	*c/a*
50	7.34	17.64	2.40
60	6.48	14.49	2.23
70	6.01	12.44	2.07
80	5.54	11.14	2.01

The only experimental technique sensitive to the phase change from the $Mh_1(0)$ to $Mh_1(R\bar{3}m)$ phase is SAXS, although figures 2 and 3 show that the phase boundaries are not sharply delineated. The traditional methods for locating phase boundaries, optical microscopy, penetration scan optical microscopy and ^{2}H NMR spectroscopy are insensitive to these mesh phase boundaries. Optical microscopy does not help because of the optical similarity of both $Mh_1(0)$ and $Mh_1(R\bar{3}m)$ phases, whilst for ^{2}H NMR, the local structures, bilayers pierced by water filled holes, are the same in both phases and the technique is insensitive to the extent of the inter-bilayer correlation. Thus the limits of the $Mh_1(R\bar{3}m)$ phase are difficult to delineate with precision. Therefore, in figure 1, the points at which observations were taken have error bars indicating the uncertainty in the boundary location.

The other phase existing in the 'lamellar' region is a disordered mesh phase, $Mh_1(0)$ of the type already reported in similar perfluorocarbon systems [10, 20]. It is characterized by the usual lamellar Bragg reflections in the ratio of 1 : 2 : 3, but with an additional broad reflection coming from water-filled holes piercing the bilayer, e.g. figure 2, 65°C or figure 3, 90% by weight. Unlike the $Mh_1(R\bar{3}m)$ phase, there is no correlation between holes in adjacent layers. In this system there may well be regions where both $Mh_1(0)$ and $Mh_1(R\bar{3}m)$ coexist in a two phase region; see for example figure 2, at 58°C where the multi-line pattern of the $Mh_1(R\bar{3}m)$ phase is weak and overlays a broad hump characteristic of $Mh_1(0)$.

Despite the difficulty in locating the boundaries between the mesh phases, it is clear from the SAXS results (figures 2 and 3) that the random mesh phase, $Mh_1(0)$ is re-entrant with respect to the $Mh_1(R\bar{3}m)$ phase. This is an indication that the structure of the $Mh_1(0)$ phase is different on the low and high surfactant concentration sides of the $Mh_1(R\bar{3}m)$ phase. At low concentrations, as the water content increases, the water layer spacing grows more rapidly than the water-filled holes in the layers, see table 3. The increased spacing between layers causes the inter-layer interaction to weaken and the correlation between the holes in adjacent layers to be lost. At high concentrations, the concentration of counter-ions in the water layer is high and this will effect the distribution of counter-ions between bulk water and the interface. Once again, this could weaken the inter-layer interaction and cause the loss of correlation, although the layer separation is now rather small.

3. Conclusions

The $Mh_1(R\bar{3}m)$ phase is unique for an ionic system; it is thermodynamically stable and covers an extensive region of the phase diagram. Its structure is similar to that observed in diblock copolymers and in non-ionic surfactant water systems. Indeed the ratio of lattice parameters $2.0 < c/a < 2.4$ is the same as that observed in the non-ionic systems [13], indicating some universality of structure even though the interactions driving the formation of the structure are very different. It is important to note that the structure of the $Mh_1(R\bar{3}m)$ phase requires a non-uniform interfacial curvature, as does the $Mh_1(0)$ phase and the nematic phase. This system shows no conventional phases with uniform interfacial curvature. It is pertinent to ask the question why this particular binary system should abhor uniform curvature. Although there is no answer to this question at the moment, it is clear that by adopting non-uniform curvature interfaces, the free energy of the system is minimized.

The detailed structure, the re-entrant behaviour and the role of the counter-ion are currently being studied and will be published when completed.

The authors would like to thank CLRC for the allocation of beamtime on line 2.1 at the Daresbury Synchrotron Source and one of us (S.P.) would like to thank the university for the award of a research studentship.

References

[1] Tanford, C., 1973, *The Hydrophobic Effect* (New York: Wiley).

[2] Fontell, K., and Lindman, B., 1983, *J. phys. Chem.*, **87**, 3289.

[3] Boden, N., Jolley, K. W., and Smith, M. H., 1993, *J. phys. Chem.*, **97**, 7678.

[4] Boden, N., Corne, S. A., and Jolley, K. W., 1987, *J. phys. Chem.*, **91**, 4092.

[5] Holmes, M. C., Smith, A. M., and Leaver, M. S., 1993, *J. de Phys. IV*, **3**, C8, 177.

[6] Vasilevskaya, A. S., Generalova, E. V., Kitaeva, E. L., and Sonin, A. S., 1988, *Russ. J. phys. Chem.*, **62**, 250.

[7] La Mesa, C., and Sesta, B., 1987, *J. phys. Chem.*, **91**, 1450.

[8] Kèkicheff, P., and Tiddy, G. J. T., 1989, *J. phys. Chem.*, **93**, 2520.

[9] HEDGE, R. M., THOMAS, R. K., MORTIMER, M., and WHITE, J. W., 1980, *J. chem. Soc., Faraday Trans. 1*, **76,** 236.

[10] FRÖBA, G., and KALUS, J., 1995, *J. phys. Chem.*, **99,** 14450.

[11] SMITH, A. M., HOLMES, M. C., PITT, A., HARRISON, W., and TIDDY, G. J. T., 1995, *Langmuir*, **11,** 4202.

[12] HOLMES, M. C., 1998, *Curr. Opin. colloid interface Sci.*, **3,** 485.

[13] FOGDEN, A., STENKULA, M., FAIRHURST, C. E., HOLMES, M. C., and LEAVER, M. S., 1998, *Prog. colloid. polym. Sci.*, **108,** 129.

[14] HAMLEY, I. W., GEHLSEN, M. D., KHANDPUR, A. K., KOPPI, K. A., ROSEDALE, J. H., SCHULZ, M. F., BATES, F. S., ALMDAL, K., and MORTENSEN, K., 1994, *J. de Phys. II*, **4,** 2161.

[15] HAMLEY, I. W., KOPPI, K. A., ROSEDALE, J. H., BATES, F. S., ALMDAL, K., and MORTENSEN, K., 1993, *Macromolecules*, **26,** 5959.

[16] HASHIMOTO, T., KOIZUMI, S., HASEGAWA, H., IZUMITANI, T., and HYDE, S. T., 1992, *Macromolecules*, **25,** 1433.

[17] FAIRHURST, C. E., HOLMES, M. C., and LEAVER, M. S., 1997, *Langmuir*, **13,** 4964.

[18] FAIRHURST, C. E., HOLMES, M. C., and LEAVER, M. S., 1996, *Langmuir*, **12,** 6336.

[19] BURGOYNE, J., HOLMES, M. C., and TIDDY, G. J. T., 1995, *J. phys. Chem.*, **99,** 6054.

[20] LEAVER, M. S., and HOLMES, M. C., 1993, *J. de Phys. II*, **3,** 105.